

Real-Time Implementation of Two Grid-Forming Power Converter Controls to Emulate Synchronous Generators

Luis Santiago Azuara-Grande
Department of Electrical Engineering
Universidad Carlos III de Madrid
Leganes, Spain
lazuara@ing.uc3m.es

Francisco Gonzalez-Longatt
Dept. of Electrical Engineering and
ICT
University of South-Eastern Norway
Porsgrunn, Norway
fglongatt@fglongatt.org

Gioacchino Tricarico
Dept. of Electrical and Information
Engineering
Polytechnic University of Bari
Bari, Italy
gioacchino.tricarico@poliba.it

Raju Wagle
Dept. of Electrical Engineering
UiT, The Arctic University of Norway
Narvik, Norway
raju.wagle@uit.no

Santiago Arnaltes
Department of Electrical Engineering
Universidad Carlos III de Madrid
Leganes, Spain
arnalte@ing.uc3m.es

Ricardo Granizo
Dept. Electrical, Electronic, Automatic
and Applied Physics
Universidad Polit cnica de Madrid
Madrid, Spain
ricardo.granizo@upm.es

Abstract—Due to climate change, progressively more isolated electrical power systems are integrating renewable energy sources. But the transition from synchronous generators to converter-interfaced generators also produces a few issues due to the lack of rotational inertia. The voltage source converters (VSCs) enabled with the so-called grid-forming control may provide a solution for the converter-dominated electrical power systems. This paper presents the implementation of two control strategies, Virtual Synchronous Machine (VSM) and Synchronverter (SynC), for converter-interfaced generators in the real-time environment (Typhoon HIL) to emulate synchronous generator (SG) behaviour. The advantages of grid-forming converter control to provide inertia response service and make the system more robust to changes in the active power of loads have been demonstrated in real-time simulations through a scenario of a positive load step connected to the converter.

Keywords—converter, grid-forming, real-time, inertia, synchronverter, Typhoon HIL

I. INTRODUCTION

Climate change and increased fuel prices have motivated a massive integration of renewable energy sources (RES) such as wind or solar. Therefore, the electricity generation using the so-called conventional non-environmentally friendly generation has been removed from the isolated electrical power systems [1]. Allowing to reduce the emissions of CO₂, have more competitive energy prices and reduce the amortization time of the investments in the electrical power systems [2]. It has been related in the scientific literature to many of the negative issues of reducing the number of synchronous machines connected to the power system, especially considering the extensive penetration of RES. Since the number of synchronous generators (SGs) connected to the power system diminishes in favour of converter-interfaced generation units, the power system inertia is reduced. However, short and long-term solutions to those challenges have been already defined in the literature; one of the long-term solutions is enabling the converter interfaced unit with a control loop to help enhance the system stability. An appropriate control technique, the converter-interfaced generators, can provide a solution to the low rotational inertia [3]. The aforementioned solution is related to controlling the converter as a voltage source converter (VSC) using the so-called grid-forming control. This approach permits to emulating of some of the electromechanical properties of the SG's behaviour.

In the scientific literature, many control techniques are reported to emulate an SG's behaviour. Many publications have proposed the concept of a Virtual Synchronous Machine (VSM) in order to simulate the SGs [3],[4],[5]. VSMs have been shown to be an excellent approach for overcoming several stability concerns and giving virtual inertia to the electrical power system [6]. Another control technique used to emulate the SGs is the innovative idea of the Synchronverter (SynC), which was proposed in [7]. SynC is a technique for controlling an inverter to imitate the behaviour of an SG. The dynamic equations are similar; only the mechanical power exchanged with the prime mover is replaced with the power exchanged with the DC bus [7].

This paper presents an implementation of two control strategies for converter-interfaced generators using a real-time simulation environment to emulate the simplified electromechanical behaviour of an SG. The implemented control strategies in this paper are the VSM and the SynC. Details of the full implementation of these VSC controllers are presented. This paper uses the Typhoon HIL framework modelling and real-time simulation. The real-time hardware-in-the-loop laboratory facility available at the DIgital Energy System laboratory –DigEnSys (<https://fglongattlab.fglongatt.org/>) has been used for this propose. The implemented grid-forming controllers have been tested using real-time simulation on a converter interfaced generation unit connected to a constant load as in an isolated grid.

The paper is organized as follows: Section II describes modelling the two grid-forming control strategies considered in this scientific paper: VSM and SynC. Section III shows an implementation of the proposed grid-forming control technique considered a converter interfaced generation unit in the form of a VSC; the implementation takes advantage of the Typhoon HIL real-time

simulation framework. Section IV gives the results of the real-time simulations. Finally, section V discusses the main conclusions of this paper.

II. MODELLING OF GRID-FORMING CONTROL TECHNIQUES

This section presents the key modelling aspects of the two grid-forming control techniques considered in this paper: VSM and SynC.

A. Virtual Synchronous Machine (VSM)

The VSM emulates the mechanical behaviour of the synchronous machine by using the swing equation below [8]:

$$\omega^* \approx \frac{1}{T_a \cdot s} P_{set} - P_{mes} - K_d(\omega^* - \omega_{set}) \quad (1)$$

where the input variable is the active power (P_{mes}) generated by VSM; the internal set values in per unit of the mechanical time constant (T_a), damping coefficient (K_d), angular frequency (ω_{set}) and active power (P_{set}); and the output variable of the angular frequency reference (ω^*). The instantaneous active (P_{mes}) and reactive power (Q_{mes}) are calculated from the measured output voltage and current ($E_{gd}, E_{gq}, I_{gd}, I_{gq}$) in the synchronous rotating frame (dq) by the following equations (2 and 3):

$$P_{mes} = E_{gd}I_{gd} + E_{gq}I_{gq} \quad (2)$$

$$Q_{mes} = E_{gd}I_{gq} - E_{gq}I_{gd} \quad (3)$$

B. Synchronverter (SynC)

The application of the electromechanical dynamic is the fundamental distinction between the Synchronverter and the VSM [9].

$$\omega^* = \frac{1}{T_a s} (T_m - T_e + D_p(\omega_{set} - \omega^*)) \quad (4)$$

$$M_f i_f = \frac{1}{K_s} (Q_{set} - Q + D_q(V_{set} - V)) \quad (5)$$

where the input variables are the electromagnetic torque (T_e), reactive power (Q) generated by Synchronverter and grid voltage (V); the internal set values in per unit of the moment of inertia (J), integrator gain (K) to regulate the field excitation, frequency droop coefficient (D_p), voltage droop coefficient (D_q), voltage (V_{set}), angular frequency (ω_{set}), active power (P_{set}) and reactive power (Q_{set}); and the output variables of the angular frequency reference (ω^*) and field excitation ($M_f i_f$). The electromagnetic torque (T_e) is the energy stored in the magnetic field of the machine by equation (6), where $\langle \cdot, \cdot \rangle$ denotes the inner product [7].

$$T_e = M_f i_f \langle i, \overline{\sin \theta} \rangle \quad (6)$$

where i_f is the imaginary field (rotor) winding of the synchronverter fed by an adjustable dc current source, $i = [i_a \ i_b \ i_c]^T$ is the stator phase currents and M_f is the mutual inductance between the field coil and each of the three stator coils [10]. The $\overline{\cos \theta}$ and $\overline{\sin \theta}$ are vectors defined as the three-phase angle difference with equal spacing of 120° or $2\pi/3$ in radian. The modulated voltage ($e = [e_a \ e_b \ e_c]^T$) is the control signal for the PWM of converter switching devices, by equation (7):

$$e = M_f i_f \omega^* \overline{\sin \theta} \quad (7)$$

The real active (P) and reactive power (Q) generated by SynC can be given by the following equations (9 and 10):

$$P = \omega^* M_f i_f \langle i, \overline{\sin \theta} \rangle \quad (8)$$

$$Q = -\omega^* M_f i_f \langle i, \overline{\cos \theta} \rangle \quad (9)$$

III. IMPLEMENTATION OF THE GRID-FORMING CONTROL TECHNIQUES

This section presents the details of the implementation of the two grid-forming control techniques using the Typhoon HIL real-time simulation framework.

A. Power network

An essential part of the implementation is the power electronic converter; in this case, the VSC implementation is shown in Fig. 1; the converter included an LC filter to reduce the harmonics at the output of the converter caused by the switching. The rest of the power network consists of a fixed load modelled as a constant impedance to simulate an isolated grid without synchronous generation.

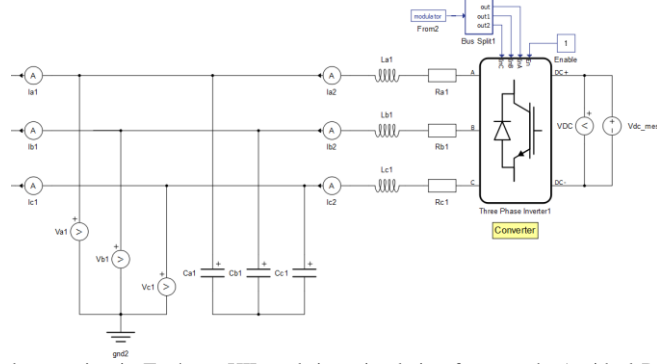


Fig. 1. Implementation of the VSC implementation in Typhoon HIL real-time simulation framework. An ideal DC source is used, and measurements are depicted.

B. Measurements and rotating dq frame

First, it is necessary to measure the required variables by the controller, as seen in Fig. 2. The input variables of the controller are the current of the inductance filter (I_{a2} , I_{b2} , I_{c2}), the voltage of the capacitor filter (V_{a1} , V_{b1} , V_{c1}) and the output LC filter current (I_{a1} , I_{b1} , I_{c1}). Also, all these variables are converted into the per-unit system to simplify the calculations inside the controller and then converted to $dq0$ rotating reference frame by the transformation block "abc to dq" from the library "core".

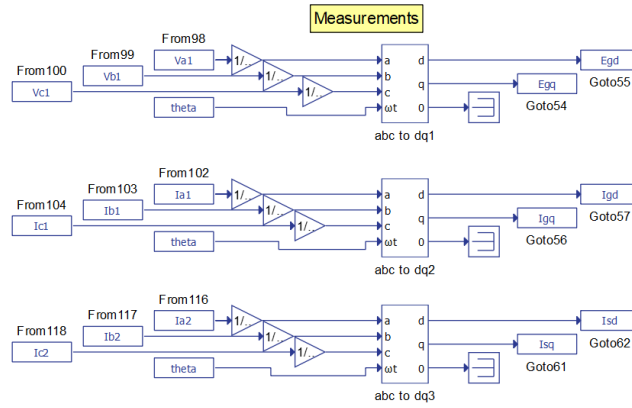


Fig. 2. Implementation of measurements in the synchronous rotating frame (dq).

C. Implementation of the VSM control technique

This section presents the implementation of VSM control strategy in the Typhoon HIL environment.

1) Active and reactive power calculations

The reactive power control loop is also known as the outer control loop (lower speed compared with the inner control loop), and it is used to regulate the voltage amplitude. The voltage magnitude reference e_{gd}^* comes from the Q - V droop control (11):

$$e_{gd}^* = V_{set} + m_q(Q_{set} - Q_{mes}) \quad (10)$$

Fig. 3 shows the active and reactive power measurements implementation in Typhoon HIL with their input variables (E_{gd} , E_{gq} , I_{gd} , I_{gq}). Also, the reactive power regulation controller implementation with the input variable of reactive power measure (Q_{mes}); the internal set values per unit of the reactive power (Q_{set}) and voltage (V_{set}); and the output variable of the voltage magnitude reference (e_{gd}^*).

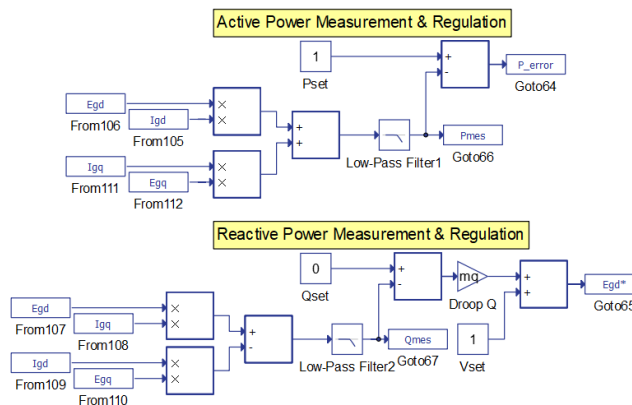


Fig. 3. Implementation of the active and reactive control loops.

2) Voltage calculations

Also known as the inner control loop, it consists of cascaded PI controllers, and its goals are the regulation of ac voltage and current. Fig. 4 shows the voltage and current controller block diagram, including all feedback (decoupling) and feed-forward terms. Both controls are achieved with a PI controller by the "PID Controller" block from the library "core". The controller has the input variables (E_{gd} , E_{gq} , I_{gd} , I_{gq}) and voltage magnitude reference (e_{gd}^*) from the reactive power regulation; the internal set value per unit of the voltage magnitude reference ($e_{gq}^* = 0$); and the output variables of the modulation voltage (e_{gd} , e_{gq}).

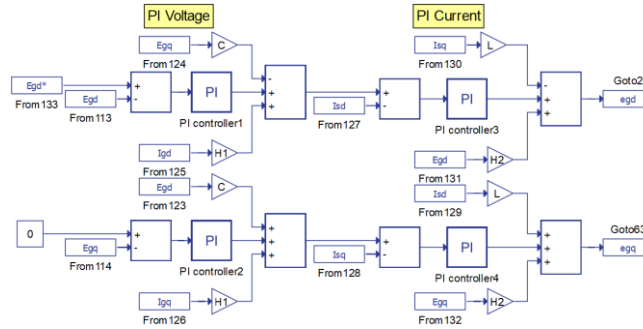


Fig. 4. Implementation of Voltage and Current Controller.

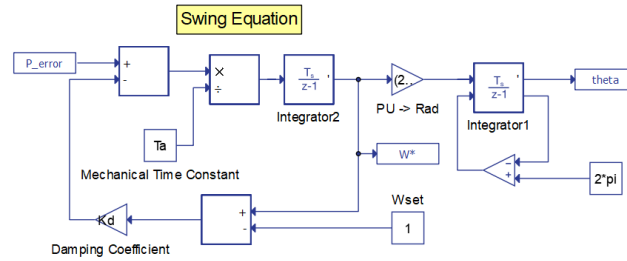


Fig. 5. Implementation of Swing Equation.

3) Electromechanical calculations

The electromechanical dynamic behaviour of the SG is simulated in the VSM as a simple swing equation, including a damping coefficient (K_d). Fig. 5 shows the implementation of the swing equation (1) with its input variable of the active power (P_{mes}) generated by VSM; the internal set values per unit of the mechanical time constant (T_a), damping coefficient (K_d), angular frequency (ω_{set}) and active power (P_{set}); and the output variable of the angular frequency reference (ω^*). The virtual rotor angular position of the VSM (θ , θ) is given by integrating the angular frequency, and this angular position corresponds to the phase angle of the voltage induced by the VSM model. In order to avoid numerical overflow, the integrator that produces θ is reset to 0 when $\theta = 2\pi$.

D. Implementation of the SynC control technique

This section presents the implementation of SynC control technique in the Typhoon HIL modelling and simulation framework.

1) Electromechanical calculations

The implementation in Typhoon HIL of the dynamic swing equations (4 and 5) is shown in Fig. 6 with their input variables of the electromagnetic torque (T_e), reactive power (Q) generated by Synchronverter and grid voltage (V); the internal set values in per unit of the mechanical time constant (T_a), integrator gain (K) to regulate the field excitation, frequency droop coefficient (D_p), voltage droop coefficient (D_q), voltage (V_{set}), angular frequency (ω_{set}), active power (P_{set}) and reactive power (Q_{set}); and the output variables of the angular frequency reference (ω^*) and field excitation ($M_f I_f$).

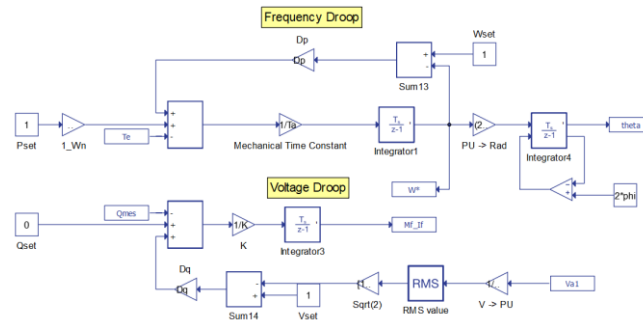


Fig. 6. Implementation of Dynamic Swing Equations.

The mechanical torque (T_m) can be obtained from the setpoint of active power (P_{set}) by dividing it by the nominal mechanical speed (ω_{set}). Again, the virtual rotor angle of the Synchronverter (θ) is given by the integral of angular frequency.

2) Trigonometric functions calculations

The $\overline{\cos \theta}$ and $\overline{\sin \theta}$ are vectors defined by (11 and 12).

$$\overline{\cos \theta} = \begin{bmatrix} \cos \theta \\ \cos \left(\theta - \frac{2\pi}{3} \right) \\ \cos \left(\theta - \frac{4\pi}{3} \right) \end{bmatrix} \quad (11)$$

$$\overline{\sin \theta} = \begin{bmatrix} \sin \theta \\ \sin \left(\theta - \frac{2\pi}{3} \right) \\ \sin \left(\theta - \frac{4\pi}{3} \right) \end{bmatrix} \quad (12)$$

3) Electromagnetic torque calculation and PWM signals

The implementation of the electromagnetic torque equation (6) is shown in Fig. 8 with their input variables of the output LC filter current (i) in per unit to simplify the controller, $\overline{\sin \theta}$ vector and field excitation ($M_f i_f$). Also, the implementation of the modulation voltage equation (7) is shown in Fig. 8 with the input variables of the $\overline{\sin \theta}$ vector, field excitation ($M_f i_f$) and angular frequency reference (ω^*).

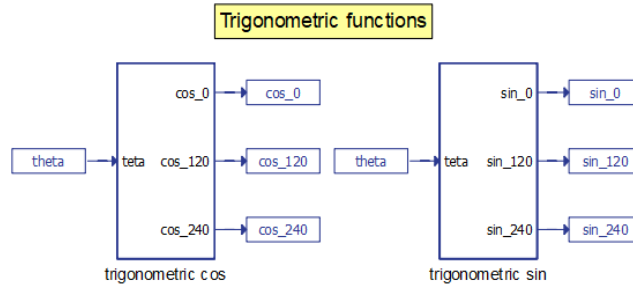


Fig. 7. Implementation of Trigonometric Functions.

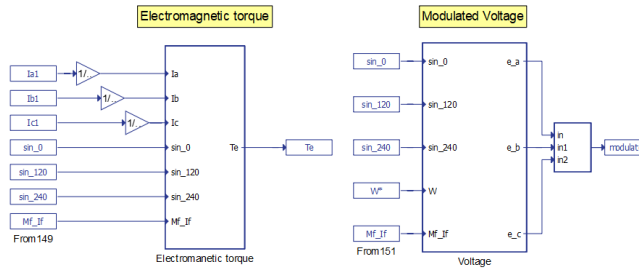


Fig. 8. Implementation of Electromagnetic Torque and Modulated Voltage.

4) Active and Reactive Power calculations

The implementation of the active and reactive power equations (8 and 9) are shown in Fig. 9 with their input variables of the output LC filter current (i) in per unit to simplify the controller, $\overline{\sin \theta}$ vector for the active power, $\overline{\cos \theta}$ vector for the reactive power, field excitation ($M_f i_f$) and angular frequency reference (ω^*).

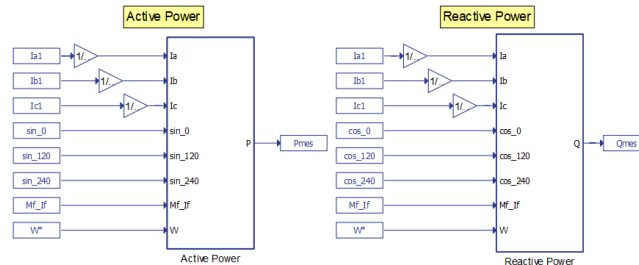


Fig. 9. Implementation of Active and Reactive Power Calculation.

IV. SIMULATION AND RESULTS

This section shows the simulation results illustrating the implemented controllers' performance using real-time simulation. The models were created using Typhoon HIL Schematic and then compiled and ran using the Typhoon HIL Scada system. The real-time simulations run in a Typhon HIL HIL604 hardware connected to a host computer.

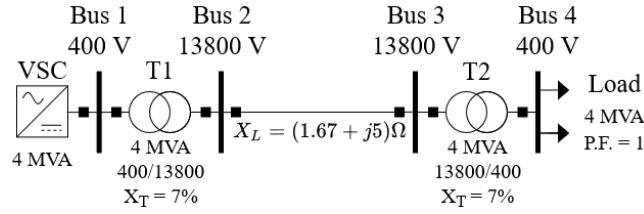


Fig. 10. Test System: Illustrative system of an isolated grid.

For illustrative purposes, a straightforward 50 Hz test system is used; it consists of a single converter interfaced generation unit connected to a fixed load through a step-up transformer (T1), one transmission line and a step-down transformer (T2) (see Fig. 10). The parameters of the models used for the grid-forming controllers implemented in this paper are shown in Table I, Table II and Table III.

TABLE I. MAIN PARAMETERS OF THE INVERTER

Description	Value
Nominal Power	4 MVA
Switching Frequency	3000 Hz
DC Link Voltage	1000 V
Resistance Filter	$0.4e-3 \Omega$
Inductance Filter	$0.0255e-3 \text{ H}$
Capacitor Filter	0.015915 F

TABLE II. MAIN PARAMETERS OF THE VSM CONTROL MODEL

Description	Variable	Value
Mechanical time constant	T_d	2 sec
Damping coefficient	K_d	100 pu
Voltage proportional gain	K_{pv}	1.00 pu
Voltage integrator gain	K_{iv}	7.80 pu
Current proportional gain	K_{pc}	1.00 pu
Current integrator gain	K_{ic}	160 pu

TABLE III. MAIN PARAMETERS OF THE SYNC CONTROL MODEL

Description	Variable	Value
Mechanical time constant	T_d	2 sec
Frequency droop coefficient	D_p	100 pu
Integrator gain	K	100 pu
Voltage droop coefficient	D_q	20 pu

To show the correct implementation of the two grid-forming control techniques, an under-frequency event is excited in the test system. The event is created by a 25% sudden step increase of the active power at the load at $t = 0.2$ secs. The plots in Fig. 11, Fig. 12, Fig. 13 and Fig. 14 capture the frequency, active power, angular frequency and electromagnetic torque response, respectively.

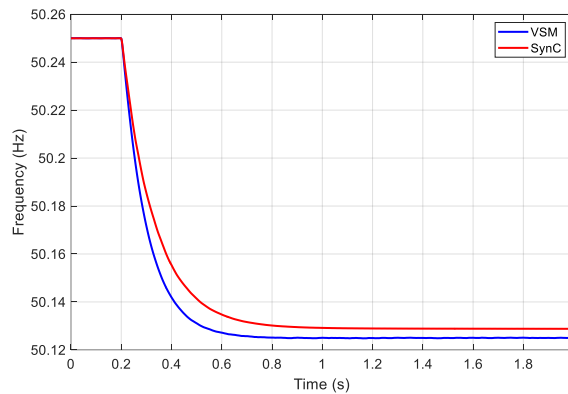


Fig. 11. Frequency response during a 25% Load Step.

The frequency response in Fig. 11 shows a different behaviour between both control strategies. The rate-of-change-of-frequency (ROCOF) for VSM control is 0.1 Hz/s while for SynC control is 0.16 Hz/s. Therefore, the frequency of the system does not suddenly drop since the inertia characteristic of an SG is emulated with both control strategies. In electrical power systems with reduced inertia or without virtual inertia integration, the ROCOF has higher values which cause larger changes in the system frequency at the same time frame.

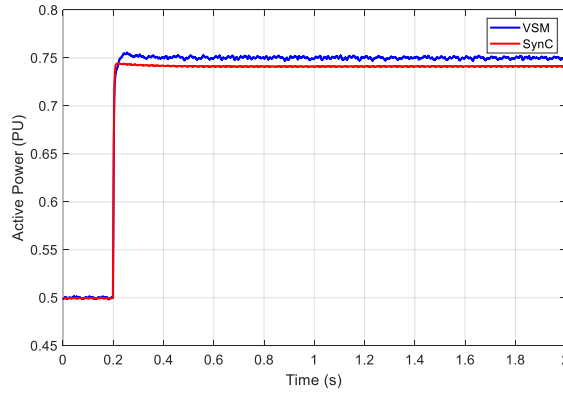


Fig. 12. Active Power response during a 25% Load Step

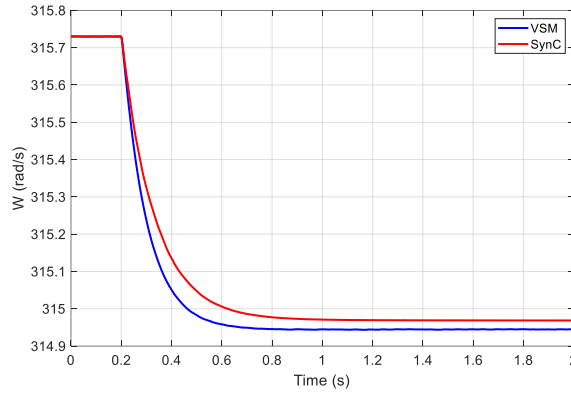


Fig. 13. Virtual Angular Frequency response during a 25% Load Step.

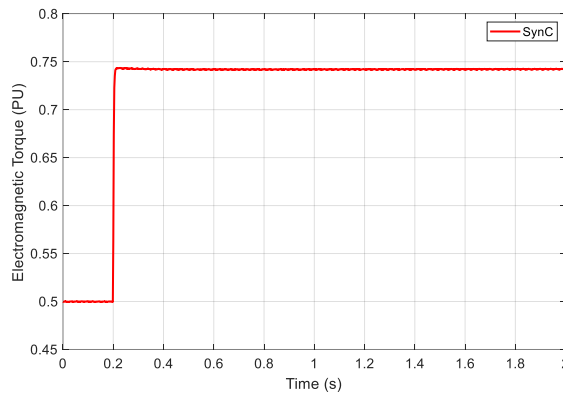


Fig. 14. Electromagnetic Torque response during a 25% Load Step.

In Fig. 12, the active power response shows a different behaviour between the two control strategies because the swing equation in VSM is expressed in terms of power instead of torque as in SynC. This difference is caused by the relationship between power and torque dependent on angular speed. As mentioned above, the difference in power is due to the difference in virtual angular speed reflected in Fig. 13. Therefore, a higher angular speed of the SynC causes its active power to be lower compared to the VSM, with a lower virtual angular speed. Fig. 14 shows that in SynC control, the mechanical torque is a control input in the swing equations since the active power and electromagnetic torque figures for SynC are the same.

V. CONCLUSIONS

This paper fully implements the VSM and SynC control strategies for converter-interfaced generators in the real-time environment (Typhoon HIL) to emulate SG behaviour in isolated grids without synchronous generation through the integration of virtual inertia into the power system by both control strategies. Therefore, emulating the behaviour of SGs by controlling VSCs with these control strategies is being recognized as an effective method for addressing potential stability issues by adding virtual inertia to the electrical power system. Future works will involve the behaviour in real-time of these control strategies during short circuits.

REFERENCES

- [1] L. S. Azuara-Grande, S. Arnaltes, J. Alonso-Martinez, and J. L. Rodriguez-Amenedo, "Comparison of two energy management system strategies for real-

- time operation of isolated hybrid microgrids," *Energies*, vol. 14, no. 20, p. 6770, 2021, doi: 10.3390/en14206770.
- [2] L. S. Azuara-Grande, S. Arnaltes, J. Alonso-Martinez, and J. L. Rodriguez-Amenedo, "EMS for fuel saving in an isolated hybrid system (solar/diesel/battery)," 2020. doi: 10.1109/EEEIC/ICPSEurope49358.2020.9160853.
- [3] S. D'Arco, J. A. Suul, and O. B. Fosso, "A Virtual Synchronous Machine implementation for distributed control of power converters in SmartGrids," *Electr. Power Syst. Res.*, vol. 122, pp. 180–197, 2015, doi: 10.1016/j.epsr.2015.01.001.
- [4] H. P. Beck and R. Hesse, "Virtual synchronous machine," *2007 9th Int. Conf. Electr. Power Qual. Util. EPQU*, 2007, doi: 10.1109/EPQU.2007.4424220.
- [5] Y. Chen, R. Hesse, D. Turschner, and H. P. Beck, "Comparison of methods for implementing virtual synchronous machine on inverters," *Renew. Energy Power Qual. J.*, vol. 1, no. 10, pp. 734–739, 2012, doi: 10.24084/repqj10.453.
- [6] A. P. Asensio, S. A. Gomez, J. L. Rodriguez-Amenedo, and M. A. Cardiel-Alvarez, "Reactive power synchronization method for voltage-sourced converters," *IEEE Trans. Sustain. Energy*, vol. 10, no. 3, pp. 1430–1438, Jul. 2019, doi: 10.1109/TSTE.2019.2911453.
- [7] Q. C. Zhong and G. Weiss, "Synchronverters: Inverters that mimic synchronous generators," *IEEE Trans. Ind. Electron.*, vol. 58, no. 4, pp. 1259–1267, 2011, doi: 10.1109/TIE.2010.2048839.
- [8] S. D'Arco and J. A. Suul, "Virtual synchronous machines - Classification of implementations and analysis of equivalence to droop controllers for microgrids," *2013 IEEE Grenoble Conf. PowerTech, POWERTECH 2013*, pp. 1–7, 2013, doi: 10.1109/PTC.2013.6652456.
- [9] K. Y. Yap, C. R. Sarimuthu, and J. M. Y. Lim, "Virtual inertia-based inverters for mitigating frequency instability in grid-connected renewable energy system: A Review," *Appl. Sci.*, vol. 9, no. 24, 2019, doi: 10.3390/app9245300.
- [10] M. Habibullah, F. Gonzalez-Longatt, M. N. Acosta Montalvo, H. R. Chamorro, J. L. Rueda, and P. Palensky, "On short circuit of grid-forming converters controllers: A glance of the dynamic behaviour," *2021 IEEE PES Innov. Smart Grid Technol. Conf. - Lat. Am. ISGT Lat. Am. 2021*, 2021, doi: 10.1109/ISGTLatinAmerica52371.2021.9543017.